



Published in final edited form as:

*Biomaterials*. 2007 October ; 28(29): 4277–4293.

## Interactive effects of surface topography and pulsatile electrical field stimulation on orientation and elongation of fibroblasts and cardiomyocytes

Hoi Ting Heidi Au<sup>1</sup>, Irene Cheng<sup>1</sup>, Mohammad Fahad Chowdhury<sup>1</sup>, and Milica Radisic<sup>1,2,3</sup>

<sup>1</sup>Department of Chemical Engineering and Applied Chemistry

<sup>2</sup>Institute of Biomaterials and Biomedical Engineering

<sup>3</sup>Heart & Stroke/Richard Lewar Centre of Excellence

### Abstract

In contractile tissues such as myocardium, functional properties are directly related to the cellular orientation and elongation. Thus, tissue engineering of functional cardiac patches critically depends on our understanding of the interaction between multiple guidance cues such as topographical, adhesive or electrical. The main objective of this study was to determine the interactive effects of contact guidance and electrical field stimulation on elongation and orientation of fibroblasts and cardiomyocytes, major cell populations of the myocardium. Polyvinyl surfaces were abraded using lapping paper with grain size 1 to 80 $\mu$ m, resulting in V-shaped abrasions with the average abrasion peak-to-peak width in the range from 3 to 13 $\mu$ m, and the average depth in the range from 140nm to 700nm (AFM). The surfaces with abrasions 13 $\mu$ m wide and 700nm deep, exhibited the strongest effect on neonatal rat cardiomyocyte elongation and orientation as well as statistically significant effect on orientation of fibroblasts, thus they were utilized for electrical field stimulation. Electrical field stimulation was performed using a regime of relevance for heart tissue *in vivo* as well as for cardiac tissue engineering. Stimulation (square pulses, 1ms duration, 1Hz, 2.3V/cm or 4.6V/cm) was initiated 24hr after cell seeding and maintained for additional 72hr. The cover slips were positioned between the carbon rod electrodes so that the abrasions were either parallel or perpendicular to the field lines. Non-abraded surfaces were utilized as controls. Field stimulation did not affect cell viability (live/dead staining). The presence of a well developed contractile apparatus in neonatal rat cardiomyocytes (staining for cardiac Troponin I and actin filaments) was identified in the groups cultivated on abraded surfaces in the presence of field stimulation. Overall we observed that i) fibroblast and cardiomyocyte elongation on non-abraded surfaces was significantly enhanced by electrical field stimulation ii) electrical field stimulation promoted orientation of fibroblasts in the direction perpendicular to the field lines when the abrasions were also placed perpendicular to the field lines and iii) topographical cues were a significantly stronger determinant of cardiomyocyte orientation than the electrical field stimulation. The orientation and elongation response of cardiomyocytes was completely abolished by inhibition of actin polymerization (Cytochalasin D) and only partially by inhibition of phosphatidylinositol 3 kinase (PI3K) pathway (LY294002).

---

Correspondence to: Milica Radisic, Ph.D. Assistant Professor Institute of Biomaterials and Biomedical Engineering Department of Chemical Engineering and Applied Chemistry Heart & Stroke/Richard Lewar Centre of Excellence University of Toronto 164 College St, Rm.407 Toronto, Ontario M5S 3G9 milica@chem-eng.utoronto.ca Phone: 416-946-5295 Fax: 416-978-4317.

**Publisher's Disclaimer:** This is a PDF file of an unedited manuscript that has been accepted for publication. As a service to our customers we are providing this early version of the manuscript. The manuscript will undergo copyediting, typesetting, and review of the resulting proof before it is published in its final citable form. Please note that during the production process errors may be discovered which could affect the content, and all legal disclaimers that apply to the journal pertain.

## Keywords

cardiomyocyte; fibroblast; surface topography; electrical stimulation; actin; cardiac tissue engineering; cell spreading

---

## 1. Introduction

Tissue engineering of functional cardiac patches critically depends on our ability to achieve appropriate structural organisation of cardiomyocytes and fibroblasts, two major cell populations found in the native myocardium. Orientation and elongation of these cells is governed by a number of cues, including electrical and topographical cues. Understanding the individual and interactive effects of these cues will ultimately enable design of improved tissue culture systems.

In previous studies, it has been shown that embryonic fibroblasts cultivated in DC electric field oriented perpendicular to the electric field lines and migrated towards the cathodal end of the field [1]. Chronic supra-threshold electrical field stimulation of cardiomyocytes in 2D was shown to preserve contractility [2], maintain calcium transients [3], promote hypertrophy [4], increase protein synthesis [5,6] and maintain action potential duration and maximum capture rate [7]. The beneficial effects of field stimulation were dependent on the occurrence of contraction following field stimulated excitation, as evidenced by the lack of observed effects in the presence of excitation-contraction decouplers: verapamil or 2,3-butanedione monoxime [8]. In 3D studies we demonstrated [9], that electrical field stimulation can be used to engineer functional cardiac tissue expressing hallmarks of cardiac differentiation. Stimulated constructs had thick elongated and aligned myofibers expressing cardiac markers, in contrast to non stimulated constructs that contained round cells [9]. Importantly, the collagen scaffold used in these studies had isotropic pore structure, thus no preferential topographical cues were provided for guidance of cellular orientation and elongation.

Microstructured grooves were used previously in 2D to direct orientation and elongation of fibroblasts [10-13]. The process was dependent upon the orientation of actin cytoskeleton [12] that also oriented along the direction of the grooves. Nuclear deformation and elongation was linked to the changes in gene expression on microstructured surfaces [14]. Elongated cardiomyocyte phenotype and alignment was achieved by cultivating cardiomyocytes on microtextured silicone membranes [15-17] that were in some cases microfluidically patterned with extracellular matrix molecules [18]. Topographical cues or micro-contact printing of extracellular matrix components were previously used to improve tissue engineering of cardiac patches. Entcheva and colleagues [19] used electrospinning to fabricate oriented biodegradable non-woven poly(lactide) (PLA) scaffolds that guided cardiomyocyte orientation. The orientation and cardiomyocyte phenotype could also be improved by microcontact printing of extracellular matrix components (e.g. laminin) on thin polyurethane and PLA films [20,21].

Yet, the interaction of topographical cues and pulsatile electrical field stimulation on the phenotypic changes in fibroblasts and cardiomyocytes has not been studied. The main objective of this study was to determine the interactive effects of contact guidance and electrical field stimulation on elongation and orientation of fibroblasts and cardiomyocytes, the major cell populations of myocardium. The cells were cultivated on 2D abraded surfaces and field stimulated using regime of relevance for heart tissue *in vivo* as well as for cardiac tissue engineering (square supra-threshold pulses, 1ms duration, 1Hz). We hypothesized that the same molecular pathways may be involved in cellular response to both cues and performed pharmacologic studies to assess the relevance of actin cytoskeleton and phosphatidylinositol 3 kinase (PI3K) pathway. Our findings indicate that contact guidance more strongly determined

cellular orientation in both cell types than electrical field stimulation, while elongation on non-abraded surfaces could effectively be modulated by electrical field stimulation.

## 2. Materials and methods

### 2.1 Microabraded surfaces

Microrstructured surfaces were prepared using the method previously described for cultivation of cardiomyocytes by Bursac et al [22]. Polyvinyl carbonate cover slips (22mm × 22mm) were abraded using lapping paper with various abrasion grain sizes from McMaster-Carr (aluminum oxide 30, 40, 60, 80µm) and Ultratech USA (silicone carbide 1, 3, 5, 9, 12µm). One half of the cover slip was abraded in one direction and the other half of the cover slip was abraded in the perpendicular direction in order to observe the cells' response to two different topographical cues on the same cover slip. The control surfaces were left non-abraded. Particulate debris was removed by sonicating (Misonix Ultrasound cleaner, model 1510R-MT) the surfaces in soap and water followed by rinsing in distilled water. The surfaces were sterilized in 95% ethanol for 24hr, followed by drying and UV irradiation for 30min. For cardiomyocyte culture, the surfaces were coated with 25µg/ml of bovine fibronectin in PBS for 2hr [22] to enhance cell attachment.

### 2.2. Cells

NIH3T3 fibroblasts were cultivated in T-75 flasks in Dulbecco's Modified Eagle Medium (DMEM) containing 4.5g/L glucose, supplemented with 10% v/v fetal bovine serum (FBS), 1% v/v of N-2-hydroxyethylpiperazine-N-2ethanesulfonic acid (HEPES) (Gibco), and penicillin-streptomycin (Gibco, 100 units/mL and 100 µg/mL respectively,). Cells were subcultured and passaged as they reached 80% confluency, typically every 3 to 4 days.

Cardiomyocytes were obtained from the hearts of 2 day neonatal Sprague-Dawley rats as in our previous studies [23-25] and according to the protocol approved by the University of Toronto Committee on Animal Care. Briefly, the hearts were quartered and incubated overnight at 4°C in a 0.06 % (w/v) solution of trypsin (Sigma) in freshly prepared Hank's balanced salt solution (HBSS) (Gibco). Subsequently, the hearts were subjected to a series of 5 digestions (8mins, 37°C, 70 rpm) in collagenase type II (Worthington, 220units/mL) in HBSS. The cell suspension was then pre-plated for 60mins to enrich for cardiomyocytes. Cell count and viability were determined via trypan blue exclusion using a hemocytometer. Culture medium was the same for NIH 3T3 fibroblasts.

### 2.3 Cell culture

For experiments without electrical field stimulation, we followed the procedure developed by Bursac et al [26]. Briefly, the abraded cover slips were cut into circular discs of 15mm diameter and placed in a 24-well tissue culture plate (1 cover slip/well). The fibroblasts (100,000 cells per disc) and cardiomyocytes (50,000 cells per disc) were seeded in 1mL of culture media. The cells were cultured in a 37°C, 5% CO<sub>2</sub> incubator for one week. The culture medium was replaced by 100% every other day.

The electrical stimulation chamber setup was based on the one we developed previously [9]. The cells were placed in between two carbon electrodes (Ladd Research Industries) that were held 1cm apart via a polycarbonate holder positioned in a 100mm by 15mm glass Petri dish. The electrodes were connected via Platinum wires to the programmable stimulator (Grass s88x, Astromed, Longueuil, QC).

For electrical stimulation experiments, the abraded cover slips (described in 2.1) were cut into 8mm by 22mm rectangles and then, folded along the two shorter edges to form a construct

resembling a table with a surface area of  $8 \times 10 \text{ mm}^2$ . The purpose of folding the cover slips was to ensure that the cells cultured on the cover slips were placed at the identical height in the center between the carbon electrodes used for electrical stimulation. Each chamber contained four cover slips; two cover slips with one half of the abrasions parallel and the other half perpendicular to the electrodes and two non-abraded cover slips to serve as controls (Supplemental Figure 1). The fibroblasts and cardiomyocytes (20,000 cells and 500,000 cells per cover slip, respectively) were seeded using  $60 \mu\text{L}$  of culture medium for 60min, followed by addition of 30ml of culture medium. The cells were cultivated for 24hr without electrical field stimulation in order to allow the cells to attach, followed by electrical field stimulation for additional 72hr using square monophasic pulses, 1ms duration and 1Hz. In preliminary studies, excitation threshold for cardiomyocytes after 24hr in culture was determined to be 2.3V/cm. Electrical field stimulation conditions were selected to correspond to the excitation threshold (2.3V/cm), and 200% of excitation threshold (4.6V/cm) to ensure that all cells, and not just most excitable cells are contracting in response to field stimulation. The control group was not stimulated (0.0V/cm). The desired stimulation regime was confirmed using oscilloscope. The medium pH was maintained during culture; no observable gas formation occurred. There were 3 independent experiments with total of N=6 samples per group.

### 2.3 Pharmacologic studies

To explore the mechanism of the cells' response to topographical cues and electrical field stimulation we treated cardiomyocytes during cultivation with Cytochalasin D ( $2 \mu\text{M}$ , Sigma) an inhibitor of actin polymerization, or LY294002 ( $50 \mu\text{M}$ , Sigma) a blocker of PI3K pathway. The drugs were applied to cardiomyocytes 24hr after seeding and they were maintained in the culture medium for the duration of the experiment (additional 72hr). Electrical field stimulation using monophasic square pulses 1ms duration, 1Hz and 4.6V/cm was initiated 24hr after seeding (upon the addition of pharmacological agents). Non-stimulated samples (0.0V/cm) served as controls. The abraded surfaces were placed in the chamber with abrasions parallel to the field lines. Two independent experiments were conducted with total of N=3 independent samples per group.

### 2.4 Assessments

**2.4.1 Scanning electron microscopy (SEM)**—Cell-free abraded cover slips were sonicated in soap water (Misonix Ultrasound cleaner, model 1510R-MT) to remove dust and debris, the samples were sputter coated with gold and imaged via SEM (Hitachi S-570) with a backscatter detector.

**2.4.2 Atomic force microscopy (AFM)**—Tapping mode AFM (TMAFM) images of surfaces abraded using lapping paper with 1, 2, 9, 12 40 and  $90 \mu\text{m}$  grain size were acquired in ambient air on a Veeco Multimode SPM (Santa Barbara, CA) equipped with a “J” scanner ( $150 \times 150 \mu\text{m}$  maximum lateral scan area), using  $125 \mu\text{m}$  long PPP-NCH Nanosensors (NanoWorld AG, Neuchatel, Switzerland). The images were captured at a frequency of  $\sim 280\text{kHz}$  and adjusted for individual cantilever. All AFM images were collected with a resolution of  $512 \times 512$  pixel, at scan rates of 1Hz. All images were flattened and plane fitted using the Nanoscope IIIa version 4.42r9 (Veeco, Santa Barbara, CA). For each grain size, 2 independent surfaces were imaged. At each surface 2 to 3 independent regions of 20, 40 or  $60 \mu\text{m}$  wide and 512 lines high were captured. Abrasion width and depth were determined with the Nanoscope IIIa version 4.42r9 software on cross-sectional profiles of the captured AFM images (Supplemental Figure 1B). Total of N=20-30 data points were collected for each grain size. The number of abrasions was manually counted in each AFM image, and divided by the width of the image in microns (20, 40, or  $60 \mu\text{m}$  width) to determine the abrasion density.

**2.4.3 Cell staining and microscopy**—Fibroblasts cultured on abraded cover slips were fixed in 10% formalin and stained with Giemsa stain (Sigma-Aldrich, 0.4 % (w/v) in buffered methanol solution), by incubating the cover slips in the stain for 5mins. Live/dead staining of cardiomyocytes and stimulated fibroblasts was performed using CFDA (live, green) and PI (dead, red) (CFDA = Carboxyfluorescein Diacetate, Succinimidyl Ester, 10 $\mu$ M ; PI = Propidium iodide, 75 $\mu$ g/mL Molecular Probes) according to the manufacturer's protocol, followed by imaging on a fluorescence microscope (Leica DMIRE2). Actin cytoskeleton of cardiomyocytes was visualized by staining with phalloidin-TRITC (50 $\mu$ g/ml) according to the manufacturer's instructions (Sigma).

Immunofluorescent staining for cardiac troponin I (contractile protein of cardiomyocytes), vimentin (intermediate filament marker for fibroblasts) and connexin-43 (gap junctional protein) was performed as described previously [9]. The dilution factors for primary antibodies were as follows: mouse anti-Vimentin Cy-3 conjugated (Sigma) at 1:75, rabbit anti-cardiac Troponin I (Chemicon) at 1:100 and rabbit anti-connexin-43 (Chemicon) at 1:50. Images were taken using the fluorescence microscope (Leica DMIRE2).

**2.4.4 Image analysis**—ImageJ software was used to determine cell alignment and elongation. Cell alignment was determined from live/dead stained images by measuring the angle between the abrasion and the long axis of the cell. Region of interest in the images was enlarged until the cell outlines (bright green) were clearly visible. For each fluorescent image, a corresponding bright field image was taken in order to determine abrasion direction relative to the long axis of the cell. Elongation was determined by measuring the long and short axes of the cell and calculating the aspect ratio (long to short axis ratio). Cells of which the perimeters could not be precisely determined were excluded from the analysis (~10%). For cells that were cultured on non-abraded surfaces, the angle between the cell's long axis and either the axis that was perpendicular (for fibroblasts) or parallel (for cardiomyocytes) to the electric field was measured. These direction were selected based on the previous studies that have demonstrated that fibroblasts aligned perpendicular to the electric field [1], while cardiomyocytes aligned parallel to the electric field [9].

**2.4.5 Excitation threshold and maximum capture rate for cardiomyocytes**—We determined the contractile function of the cardiomyocytes by measuring the excitation threshold (ET) and maximum capture rate (MCR) before and after the electrical stimulation period as described in our previous studies [24]. ET was defined as a minimum voltage required to induce synchronous contractions of at least 75% of the cells in the field of view using monophasic pulses 2ms duration and 1Hz. MCR was defined as a maximum beating frequency at 200% of ET. The measurement was performed at room temperature in culture medium using a tissue culture microscope (Olympus CKX41).

## 2.5 Statistical analysis

Tests for normality and equality of variance were performed on all data sets. For data that were normally distributed and with equal variance we performed one-way ANOVA in conjunction with Student-Newman-Keuls test for pairwise comparisons. Otherwise, Kruskal-Wallis one-way ANOVA on ranks was utilized followed by pairwise comparisons using Dunn's test (Sigma Sat 3.0). The significance level for all tests were  $P < 0.05$ .

## 3. Results

### 3.1 Abraded surfaces as a model system for study of topographical cues

Abraded surfaces with topographic cues of the micron size were prepared on polyvinyl cover slips by the previously described method [22], using a lapping paper with grain size in the

range of 1 to 80 $\mu$ m. Scanning electron microscopy demonstrated that with the increased grain size, the width and the depth of the abrasions obtained on the surface increased (Figure 1A, B) while abrasion density decreased (Figure 1C). AFM analysis indicated that the abrasions were V-shaped, although they were significantly less uniform than abrasions prepared previously by micromachining [27,28] and microfabrication [17] techniques.

Although all abraded surfaces qualitatively improved the elongation of NIH 3T3 fibroblasts (Figure 2A, B, C and, Supplemental Figure 2) as measured by the ratio of long axis to the short axis (aspect ratio), the effect was statistically significant (compared to non-abraded) for the surfaces with the abrasion abraded with grain size 30-60 $\mu$ m (average width from 9.7 to 13 $\mu$ m, and depth from 640 to 700nm). Box plots were utilized to represent cellular orientation, since on abraded surfaces cells cluster around a low orientation angle, i.e. the angle distribution is not Gaussian. In box plots, the line in the middle of the box defines the median value; the ends of the boxes define the 25th and 75th percentiles, and error bars defining the 10th and 90th percentiles. Fibroblasts cultivated on non-abraded surfaces had a random distribution (Figure 2 A, C). The surfaces abraded with grain size from 9 to 80 $\mu$ m significantly improved cell orientation along the direction of the grooves compared to the non-abraded controls.

Cultivation on abraded surfaces resulted in high viability in all groups (live/dead staining, Figure 2D) **and a** statistically significant effect on elongation (aspect ratio, Figure 2E). Cardiomyocytes cultivated on the surfaces abraded with lapping paper of grain size 40  $\mu$ m and 80  $\mu$ m were significantly more elongated (Figure 2E) and aligned (Figure 2F) than those cultivated on non-abraded surfaces. Since surfaces abraded with lapping paper of 80  $\mu$ m grain size (average abrasion width of 13 $\mu$ m and depth of 700nm) exhibited the strongest effect on cardiomyocyte elongation and orientation as well as statistically significant effect on orientation of fibroblasts, they were used for electrical field stimulation experiments. The non-abraded polyvinyl cover slips served as controls.

### 3.2 Interactive effects of contact guidance and electrical field stimulation on fibroblasts and cardiomyocytes

Electrical field stimulation did not have any adverse effects on viability of fibroblasts (Supplemental Figure 3) and cardiomyocytes (Supplemental Figure 4) as indicated by majority of green (live) cells in the live/dead staining. At low voltage (0.0 and 2.3V/cm) fibroblasts were significantly more elongated on abraded compared to non-abraded surfaces (Figure 3A, stars). Yet, at 4.6V/cm there was no statistically significant difference in the elongation of fibroblasts cultivated on abraded vs. non-abraded surfaces, due to the fact that elongation on non-abraded surfaces increased significantly in the stimulated groups (Figure 3A, white bars).. Fibroblasts cultivated on abraded surfaces were also significantly more aligned (smaller angle, Figure 3B) compared to those cultivated on non-abraded surfaces at all field strengths (0.0V/cm, 2.3V/cm and 4.6V/cm). Yet, electrical field stimulation significantly enhanced the alignment of fibroblasts on abrasions that were placed perpendicular to the field lines (Figure 3B, light-grey bars). This result is consistent with previously reported findings that fibroblasts preferentially orient perpendicular to the field lines in DC fields [1]. For fibroblasts cultivated on non-abraded surfaces, there was a qualitative shift in orientation angle towards the direction perpendicular to the field lines at the highest field strength investigated (4.6V/cm) (Figure 3B white bars).

Overall we observed two effects of the field stimulation on fibroblasts: i) fibroblast elongation on non-abraded surfaces was significantly enhanced by electrical field stimulation and ii) electrical field stimulation promoted orientation of fibroblasts in the direction perpendicular to the field lines when the abrasions were also placed perpendicular to the field lines.

We observed similar effects of the field stimulation on the elongation of cardiomyocytes as a function of topographical cues (Figure 3C). At 0.0V/cm and 2.3V/cm, cardiomyocytes were significantly more elongated on abraded surfaces compared to the non-abraded surfaces (Figure 3C, stars), while there was no significant difference at 4.6V/cm. Specifically, cardiomyocyte elongation on non-abraded surfaces increased significantly at the highest field strength and became comparable to that of abraded surfaces (Figure 3C, white bars). Topographical cues had significantly stronger effect on cardiomyocyte orientation. At all field strengths investigated, the abraded surfaces had significantly smaller average orientation angle compared to the non-abraded surfaces, (Figure 3D). There was a slight, but not significant, decrease of the orientation angle on non-abraded surfaces (Figure 3D, white bars) stimulated at 4.6V/cm, indicating that the cells may be starting to orient parallel to the field lines.

Overall we observed that i) cardiomyocyte elongation on non-abraded surfaces was significantly enhanced by electrical field stimulation ii) topographical cues were a significantly stronger determinant of cardiomyocyte orientation than the electrical field stimulation.

### 3.3 Presence of cardiac markers and contractile properties

The cell phenotype was validated by immunostaining for phenotypic markers vimentin for fibroblasts (data not shown), and troponin I for cardiomyocytes (Figure 4). Presence of connexin-43, a gap junctional protein required for electrical communication between the cells was also documented (Supplemental Figure 6). Morphometry following immunostaining for cardiac Troponin I, indicated that 97-99% of cells on the surfaces were cardiomyocytes. Cross-striations in individual cardiomyocytes were generally oriented perpendicular to the abrasion direction (Figure 4) with a remarkably well developed contractile apparatus for cells cultivated at 4.6V/cm on surfaces with abrasions perpendicular to the field lines (Figure 4B). On non-abraded surfaces, there was no preferential directionality in cross-striation orientation, due to the random cellular orientation and cross-striations present only in the short domains (Figure 4B, non-abraded).

Low magnification images of phalloidin-TRITC stained images (Figure 5A) indicated that actin filaments generally followed the direction of surface abrasions. For cells cultivated on non-abraded surfaces, actin cytoskeleton was disorganized. Higher magnification images (Figure 5B) revealed remarkable differences in orientation of actin filaments as a function of surface abrasion and electrical field stimulation. On abraded surfaces, actin filaments were clearly aligned in the direction of surface abrasions (either perpendicular or parallel to the field lines) with elements of cross-striations observable in some groups (e.g Figure 5B 2.3V/cm, perpendicular). For cardiomyocytes cultivated on non-abraded surfaces at 0.0V/cm and 2.3V/cm (Figure 5B) actin cytoskeleton was clearly disorganized, with overlapping filaments extending in multiple directions. Yet, at 4.6V/cm on non-abraded surfaces (Figure 5B), there was an appreciable improvement in the organization of the actin filaments so that they were clearly parallel and following the long axis of the cell.

Consistent with our previous data [9], we found that ET significantly decreased with time in culture for all experimental groups. At the end of cultivation, cells on abraded surfaces had slightly lower ET when cultured with field stimulation in comparison to their non-stimulated controls; on non-abraded surfaces ET was slightly increased with stimulation. Field stimulation and topographical cues had interactive effects on the MCR. Overall higher MCR was achieved with cardiomyocytes cultivated on the non-abraded surfaces compared to those cultivated on the abraded surfaces. In general, MCR decreased significantly at 72hr of culture compared to the 24hr of culture for all groups, with the exception of non-abraded and perpendicular abrasions at 2.3V/cm. At the end of cultivation, cardiomyocytes cultivated on abraded surfaces placed parallel to the field lines, exhibited a slight but significant increase in MCR with the increase of stimulation field strength from 2.3V/cm to 4.6V/cm.

### 3.4 Pharmacological studies

Pharmacological studies focused on cardiomyocytes, a cell type that is responsible for contractile function. Inhibition of actin polymerization had dramatic effects on the ability of cardiomyocytes to respond to the either topographical cues or field stimulation. Regardless of the experimental conditions the cell morphology was round, the cells appeared mono-nucleated (Supplemental Figure 5) when treated with Cytochalasin D and maintained aspect ratio of  $\sim 2$  (Figure 6A, C). They were also unable to orient, either in response to the electrical field stimulation or topography (Figure 6B, D). Yet, live/dead staining indicated no significant difference in cell viability between samples treated with Cytochalasin D and drug-free controls (Supplemental Figure 5).

Elongated cells were observed in the groups treated with LY294002. However, cell viability was significantly lower in the LY294002 treated samples compared to the drug free controls or samples treated with Cytochalasin D (Supplemental Figure 5), consistent with the well known effects of the PI3K pathway in prevention of apoptosis in cardiomyocytes [29]. When field stimulation was applied, the drug-free cardiomyocytes and those treated with LY294002 exhibited a statistically significant increase in the aspect ratio (Figure 6A, B). Specifically in non-stimulated LY294002 group, cell elongation on abraded surfaces was slightly but significantly lower than that of drug-free controls (Figure 6C). Application of field stimulation completely reversed this effect resulting in a comparable elongation in LY294002 treated cells and the controls on abraded surfaces (Figure 6C) as well as a significantly higher elongation in LY294002 treated cells compared to the drug free controls on non-abraded surfaces (Figure 6A). Blocking of PI3K pathway only partially inhibited the orientation response of cardiomyocytes (Figure 6B, D). For non-stimulated samples on abraded surfaces (Figure 6D), the average orientation angle of LY294002 treated cells was significantly larger than that of controls, but also significantly smaller compared to the Cytochalasin D treated cells. The application of electrical field stimulation (4.6V/cm) reversed this effect and resulted in the orientation levels in LY294002 groups comparable to those of drug-free controls (Figure 6D).

Overall our results indicate that blocking of actin polymerization significantly inhibited the ability of cardiomyocytes to elongate and orient in response to topographical cues or electrical field stimulation. Blocking of the PI3K pathway resulted in a partial reduction in cellular elongation and alignment on abraded surfaces. However, this reduction was reversed by the application of electrical field stimulation.

Qualitatively, overall cell morphology and contractile apparatus were most developed in the drug-free controls cultivated on abraded surfaces in the presence of electrical field stimulation (4.6V/cm). The Cytochalasin D treated cells did exhibit the presence of Troponin I (Figure 7), but a developed contractile apparatus in individual cardiomyocytes could not be identified in majority of the cells. Blocking of PI3K pathway resulted in the overall qualitative decrease in cell size compared to drug-free controls consistent with the involvement of PI3K pathway in the hypertrophic response [30] with the contractile apparatus still present in a number of cells (Figure 7).

Staining with Phalloidin-TRITC revealed dramatic differences in actin cytoskeleton (Figure 8) as a function of drug treatment. The application of Cytochalasin D completely abolished actin polymerization as demonstrated by the complete lack of microfilaments in this group regardless of the surface abrasions or electrical field stimulation (Figure 8). Cells treated with LY294002, exhibited staining for actin microfilaments with the improved cytoskeletal organization upon the application of electrical field stimulation (Figure 8). The major difference between the drug-free and LY294002 cells is that LY294002 cells assumed a more flat morphology in all groups.



At the end of cultivation the drugs were removed and we evaluated the ability of all our test groups to contract in response to electrical field stimulation. Drug-free constructs had lower ET at 72hr of culture compared to the 24hr of culture (Table 2) consistent with the results presented in Table 1. The application of either Cytochalasin D or LY294002 significantly affected the contractile response and prevented synchronous contractions of the cells. In these two groups, we only observed contractions of single randomly scattered cells.

## 4. Discussion

*In vivo* multiple guidance cues determine cell orientation and phenotype. These include topographical, adhesive, electrical, mechanical and chemical cues. The interactive effects of topographical and adhesive cues [31-33] have been studied extensively. Lesser attention was devoted to the interaction between adhesive and electrical cues [34], indicating that adhesive cues guided neurite outgrowth more strongly than electrical cues. Yet, the interaction between electrical cues and topography especially at conditions relevant for tissue engineering remained largely unstudied.

In adult myocardium, the cardiomyocytes are elongated, oriented in parallel, forming a three-dimensional syncytium that enables propagation of electrical signals. Cardiac fibroblasts are scattered amongst the myofibers, secreting components of the extracellular matrix (ECM) and transmitting mechanical force by the receptor mediated connections to the ECM [35,36]. One of the challenges of cardiac tissue engineering is reproducing the “*in-vivo-like*” orientation and elongation of the cells in an engineered cardiac patch.

The main objective of this study was to determine interactive effects of topographical cues and electrical field stimulation on cellular elongation and orientation at conditions relevant for cardiac tissue engineering. We focused on neonatal rat cardiomyocytes, a contractile cell documented to be responsive to both contact guidance [16] and electrical field stimulation [2,7]. We also studied the response of fibroblasts a non-contractile cell type with documented ability to align in response to contact guidance [37] and DC fields [1].

### 4.1 Selection of topographical cues, electrical field stimulation conditions and pharmacological agents

To introduce topographical cues (Figure 1), we used a previously established method of abrading polyvinyl cover slips using lapping paper [22,38]. Bursac et al demonstrated that these surfaces resulted in a similar degree of cardiomyocyte orientation and elongation as the surfaces prepared using microcontact printing of laminin lanes [22] and that they could be utilized as model for electrophysiological studies [22,38].

Fibroblasts and cardiomyocytes were cultivated on the surfaces with the average abrasion width ranging from 3 to 13 $\mu$ m and depth from 140 to 700nm. From these experiments a group of surfaces that elicited the most significant orientation and elongation of both cell types, in comparison to non-abraded surfaces, was selected to be further studied with electrical field stimulation. The non-abraded surfaces (corresponding to the smallest cellular orientation and elongation), were used as a control. Although *in vivo*, ECM proteins assemble into structures on the order of 10-100nm, the, guidance cues of the structures on the order of  $\mu$ m are well documented [12,39,40]. In the native rat heart, elongated cardiomyocytes are tightly positioned between capillaries (7 $\mu$ m in diameter) that are spaced  $\sim$ 20 $\mu$ m apart [41], thus structures on the order of 1-10 $\mu$ m have physiological relevance.

For electrical field stimulation we used monophasic square pulses of 1ms duration at the rate of 1Hz and field strength of 2.3 or 4.6V/cm. Stimulus pulse width corresponds to that found in the hearts of 1 week old rats [42] and the frequency of 1Hz is physiological for humans and

at the low end of physiological regime for rats. The duration of culture and selection of field intensity was consistent with previous cardiac tissue engineering studies (5V/cm, [9]) and cardiomyocyte monolayer studies (2.6V/cm, [2,7]). The selected field strengths are within the order of magnitude of the fields that occur *in vivo* [43]. Most importantly, the selected field strengths were at (2.3V/cm) or above the excitation threshold (4.6V/cm) for our cultures (Table 1) to ensure synchronous cardiomyocyte contractions. In addition, the DC fields of comparable strength were previously demonstrated to affect the alignment and orientation of fibroblasts [1].

The electrical field stimulation was initiated 24hr after cell seeding. The lag period was intended to provide the cells with enough time to recover from trypsinisation/isolation procedure and enable attachment. This lag period is also consistent with our results [9] and those of others [2] indicating that initiation of field stimulation too early in culture (less than 24hr) had detrimental effects on cellularity and failed to induce cardiomyocyte hypertrophy and improved contractile function.

It is important to note that we utilized a high cell seeding density in order to achieve confluent monolayers, as these conditions are of relevance for tissue engineering. In order to be functional, engineered cardiac constructs require a formation of syncytium at a cell density close to physiological ( $10^8$  cells/cm<sup>3</sup>). However, observing the effects of topographical cues [44] as well as electrical cues [34] is more conveniently performed at a low cell density.

For pharmacological studies we utilized Cytochalasin D and LY294002. Cytochalasin D is a fungal alkaloid that depolymerizes actin filaments by binding to the + end of F-actin thus blocking the addition of more units. It was used previously in the range of 1-40 $\mu$ M [45] to disrupt actin cytoskeleton in cardiomyocytes [46,47]. Our use of 2 $\mu$ M is consistent with those studies. LY294002 is a standard inhibitor of PI3K kinase that was used in a large number of studies at a concentration range 10-50 $\mu$ M [29,30,48]. It was documented to completely abolish PI3 kinase activity with concentration required for 50% inhibition (IC<sub>50</sub>) of 1.40 $\mu$ M [49]. Our choice of 50 $\mu$ M is consistent with those studies.

#### **4.2 Effects of surface topography and electrical field stimulation on orientation and elongation of fibroblasts and cardiomyocytes**

We observed that both fibroblasts and cardiomyocyte elongated and aligned with their axis parallel to the surface abrasions (Figure 2). The degree of alignment and elongation was significantly higher for deeper abrasions, consistent with previously reported studies that utilized grooves of precisely defined dimensions [11,44,50] as well as the rough surfaces [51]. We expect that utilizing surfaces with more uniform abrasion features, such as those that can be prepared by microfabrication [16], would decrease the spread (i.e. error bars) in the measurement of aspect ratio and the elongation angle, yet the mean values would be comparable.

The surface abrasions were placed either perpendicular or parallel to the field lines. This way the two cues (topography and field) act on the cell either in a parallel or in an orthogonal direction. Overall, our results indicated that on non-abraded surfaces, pulsatile electrical field stimulation significantly enhanced elongation of fibroblasts and cardiomyocytes to reach the levels comparable to that achieved by surface abrasion (Figure 3A, C). The fact that field stimulation failed to promote elongation at higher levels than that obtained by topographical cues, prompted us to hypothesize that the same signaling pathways may be involved in the cellular response (i.e. elongation) to topographical cues and electrical field stimulation. In addition, pulsatile electrical field stimulation significantly enhanced orientation of both of fibroblasts and cardiomyocytes when they were cultivated on abrasions placed perpendicular to the field lines (Figure 3 B, D). Yet, within every voltage group, the non-abraded surfaces

had approximately two times higher average orientation angle than the abraded surfaces (Figure 3 B, D), indicating that that topographical cues are overall stronger regulator of cellular orientation than field stimulation.

The cardiomyocytes were capable of contracting in response to electrical field stimulation (Table 1), consistent with the presence of a contractile protein cardiac Troponin I and a well developed contractile apparatus (Figure 5A). In general, cardiomyocytes exhibited a decrease in ET, most likely due to the improved cellular coupling [26] consistent with our previous studies [9].

In general, MCR either decreased (Table 1) or remained comparable at 72hr in culture compared to 24hr in culture. Previous studies reported a significant increase in the MCR in monolayers of non-stimulated cardiomyocytes (cultivated on non-abraded surfaces) with time in culture, whereas paced cardiomyocyte monolayers exhibited a slight but not significant decrease in MCR [7]. Our previous studies with cardiac tissue constructs demonstrated a significant increase in MCR with time in culture. The increase in MCR was higher for constructs cultivated with the electrical field stimulation, thus the monolayer results (Table 1) are not consistent with those observed previously for the 3D constructs. The stiffness of the underlying substrate may be a likely cause for this discrepancy. When cultured on collagen sponges, the cardiomyocytes cause macroscopic contractions of the collagen scaffold at each beat. For cells cultured on rigid polystyrene surfaces such movement of the underlying substrate is not possible, thus affecting synchronized contractions of the cells at higher frequencies.

The application of electrical field stimulation to cultured cells induces hyperpolarization at the anode end of the cell and depolarization at the cathode end of the cell [52]. The higher the field, the more likely a cell is to reach the depolarization threshold, generate action potentials and contract in response to the stimulus. It is the contraction part of this excitation-contraction coupling and active tension development that enables the assembly and maintenance of the contractile apparatus in a 2D and 3D culture of cardiomyocytes [2,4,9,53,54]. If contractions are prevented, degradation and decrease in synthesis of sarcomeric proteins occurs, a process that can be reversed by regular contractile activity [53]. Thus, regular supra-threshold electrical stimuli can be utilized to induce a hypertrophic response in cardiomyocytes [4] and enhance cellular elongation, via mechanically activated signalling pathways [8].

### 4.3 Significance of the findings

According to one hypothesis, grooved surfaces enable cellular orientation by confining cell adhesion molecules (e.g. focal adhesions) to an orientation parallel to the groove direction [12,13]. As the ridge size of the grooved surfaces is decreases (to e.g.  $\sim 2\mu\text{m}$ ) focal adhesions which are also  $\sim 2\mu\text{m}$  in width can assume only one possible orientation on the surface: the one that is parallel to the grooves. In addition, ECM proteins orient parallel to the groove direction on microstructured surfaces, affecting the orientation of integrins. Since adhesion molecules are coupled to the actin cytoskeleton, this causes the orientation of the actin filaments parallel to the groove direction [12,13], as we also observed in Figure 5. Numerous previous studies demonstrated that polymerization of F-actin is critical in cell motility and response of fibroblasts to surface topography [12,55,56]. Thus not surprisingly, we found that the disruption of actin cytoskeleton by Cytochalasin D had a detrimental effect on the ability of cardiomyocytes to elongate and orient in response to topographical as well as electrical cues (Figure 6-8).

In our experimental design, the cells were exposed to the topographical cues first, by allowing them to attach to the grooved surfaces for 24hr prior to the initiation of the pulsatile electrical field stimulation. We found that the electrical field stimulation could not reorient the cells that assumed an orientation defined by the topographical cues (Figure 3B, D). Pulsatile field

stimulation enhanced the cellular elongation (Figure 3 A, B), enabled the formation of more organized sarcomeres (Figure 4B) and improved local organization of actin cytoskeleton (Figure 5B).

Importantly, the cover slips used for cell growth were rigid and non-degradable, thus cells had no ability to remodel the substrate during cultivation. Thus, substrate remodeling may be required for cells to change their orientation in response to field stimulation. It is possible that the utilization of the higher field strength would reorient the cells on the abraded surfaces. However, higher field strength may not be a feasible approach as continuous stimulation would lead to a decrease in cell viability (Radisic, unpublished observations). It is also possible that had a different abrasion feature been chosen (e.g. nano-structured surfaces) pulsatile electrical field stimulation would be more effective at directing cellular orientation.

To control changes in cell orientation and elongation, extracellular stimuli must initiate intracellular signaling that modifies organization of the cytoskeleton. PI3-kinases take part in extracellular signal transduction by phosphorylating the hydroxyl group at positions 3 of membrane lipid phosphoinositides. The PI-3 phosphates then transduce signals downstream by acting as docking sites for a number of signal-transducing proteins (e.g. protein kinase B etc.) The PI3K pathway was documented to regulate a number of physiological functions, including cell growth, survival and actin cytoskeleton rearrangement [57]. It was documented to be involved in a physiological hypertrophy of cardiomyocytes [58,59] as well as in the response of endothelial cells [60], keratinocytes and epithelial cells to stimulation with DC fields [61]. In activated platelets, PI3-kinase associates with cytoskeleton when significant actin polymerization occurs [62]. Thus it was a logical pathway to investigate in the response of cardiomyocytes to topographical cues and pulsatile electrical field stimulation.

Inhibition of PI3K pathway significantly decreased cardiomyocyte orientation and elongation on abraded surfaces, implying a role of this pathway in response to topographical cues (Figure 6C, D). Yet pulsatile field stimulation was able to reverse this effect (Figure 6C, D), indicating that a parallel pathway may be involved in transduction of the electrical stimulation signals. Zhao et al [60] documented that in addition to PI3 kinase pathway, Rho kinase pathway was involved in the response of endothelial cells to DC field stimulation. However, LY294002 treated monolayers could not contract synchronously in response to electrical field stimulation, although both actin cytoskeleton (Figure 8) and sarcomeres (Figure 7) were identified, an observation consistent with our previous findings on cardiac tissue constructs [9].

#### 4.4 Implications of the findings for cardiac tissue engineering

Our findings indicate that orientation of fibroblasts and cardiomyocytes is primarily determined by surface topography. Thus, in order to engineer tissue with a desired cellular orientation scaffolds with anisotropic structure, such as those created by electrospinning and post-processing to achieve unidirectional fiber orientation [19,63,64] are required. Once desired cellular orientation is achieved, electrical field stimulation can be initiated 1-3 days after cell seeding on scaffolds to further modulate cellular elongation, contractile properties and organization of cytoskeletal and contractile proteins. The stimulus amplitude should be adjusted so that it surpasses the ET for synchronous contractions of the patch.

Two more approaches enable direct translation of our findings to improved methods of tissue engineering. In one approach biodegradable polymer films can be directly cast over the microstructured surfaces to obtain thin scaffolds capable of guiding cellular orientation, followed by the application of electrical field stimulation 1-3 days after cell seeding. In another approach, microstructured surfaces can be combined with cell sheet technology developed by Okano and colleagues [65] and used to stack oriented layers of cardiomyocytes. As orientation of myofibers changes along thickness of the ventricular wall, this approach could in principle

yield a patch of myofibers aligned in parallel, with orientation angles changing as a function of patch thickness to mimic that found in the native heart. Application of electrical field stimulation would then enhance the overall contractile properties of the patch, but it is not expected to significantly change the fiber orientation.

## 5. Conclusions

Taken together, our data suggest that surface topography more strongly determines orientation of fibroblasts and cardiomyocytes than pulsatile electrical field stimulation. Yet, pulsatile electrical field stimulation had appreciable effects on cellular elongation. On non-abraded surfaces electrical field stimulation significantly promoted elongation of cardiomyocytes and fibroblasts to the levels comparable to that obtained by the topographical cues. On abraded surfaces the electrical field stimulation enhanced orientation and elongation along the abrasion direction, but it could not reverse the effect of the cues provided by surface topography. The orientation and elongation response of cardiomyocytes to the abraded surfaces and electrical field stimulation was completely abolished by inhibition of actin polymerization and only partially by inhibition of PI3K pathway. These findings have significant implications for the design of scaffolds for cardiac tissue engineering. A feasible strategy would be to design scaffolds of desired microarchitecture (i.e. by electrospinning) to drive cellular elongation and orientation in the desired direction, followed by the application of electrical field stimulation for enhancement of these properties.

## Supplementary Material

Refer to Web version on PubMed Central for supplementary material.

## 6. Acknowledgements

The authors would like to thank Mr. Rohin Iyer for help with SEM, Dr. Christopher Yip and Mr. Patrick Yang for help with AFM and Dr. Gordana Vunjak-Novakovic for constructive review of the manuscript. This work was supported by the grants from National Science and Engineering Research Council (NSERC DG), Canada Foundation for Innovation (Leaders Opportunity Fund), Ontario Research and Development Challenge Fund (ARTEC), NIH grant R01HL076485 and University of Toronto Open Fellowships to HTHA and MFC.

## 8. References

1. Erickson CA, Nuccitelli R. Embryonic fibroblast motility and orientation can be influenced by physiological electric fields. *J Cell Biol* 1984;98:296–307. [PubMed: 6707093]
2. Berger HJ, Prasad SK, Davidoff AJ, Pimental D, Ellingsen O, Marsh JD, et al. Continual electric field stimulation preserves contractile function of adult ventricular myocytes in primary culture. *Am J Physiol* 1994;266:H341–9. [PubMed: 8304516]
3. Holt E, Lunde PK, Sejersted OM, Christensen G. Electrical stimulation of adult rat cardiomyocytes in culture improves contractile properties and is associated with altered calcium handling. *Basic Res Cardiol* 1997;92:289–98. [PubMed: 9486350]
4. Johnson TB, Kent RL, Bubolz BA, McDermott PJ. Electrical stimulation of contractile activity accelerates growth of cultured neonatal cardiocytes. *Circ Res* 1994;74:448–59. [PubMed: 8118953]
5. Ivester CT, Tuxworth WJ, Cooper Gt, McDermott PJ. Contraction accelerates myosin heavy chain synthesis rates in adult cardiocytes by an increase in the rate of translational initiation. *J Biol Chem* 1995;270:21950–7. [PubMed: 7665617]
6. Kato S, Ivester CT, Cooper Gt, Zile MR, McDermott PJ. Growth effects of electrically stimulated contraction on adult feline cardiocytes in primary culture. *Am J Physiol* 1995;268:H2495–504. [PubMed: 7611500]
7. Sathaye A, Bursac N, Sheehy S, Tung L. Electrical pacing counteracts intrinsic shortening of action potential duration of neonatal rat ventricular cells in culture. *J Mol Cell Cardiol* 2006;41:633–41. [PubMed: 16950369]

8. Strait JB, Samarel AM. Isoenzyme-specific protein kinase C and c-Jun N-terminal kinase activation by electrically stimulated contraction of neonatal rat ventricular myocytes. *J Mol Cell Cardiol* 2000;32:1553–66. [PubMed: 10900180]
9. Radisic M, Park H, Shing H, Consi T, Schoen FJ, Langer R, et al. Functional assembly of engineered myocardium by electrical stimulation of cardiac myocytes cultured on scaffolds. *Proc Natl Acad Sci U S A* 2004;101:18129–34. [PubMed: 15604141]
10. Vernon RB, Gooden MD, Lara SL, Wight TN. Microgrooved fibrillar collagen membranes as scaffolds for cell support and alignment. *Biomaterials* 2005;26:3131–40. [PubMed: 15603808]
11. Flemming RG, Murphy CJ, Abrams GA, Goodman SL, Nealey PF. Effects of synthetic micro- and nano-structured surfaces on cell behavior. *Biomaterials* 1999;20:573–88. [PubMed: 10213360]
12. den Braber ET, de Ruijter JE, Ginsel LA, von Recum AF, Jansen JA. Orientation of ECM protein deposition, fibroblast cytoskeleton, and attachment complex components on silicone microgrooved surfaces. *J Biomed Mater Res* 1998;40:291–300. [PubMed: 9549624]
13. den Braber ET, de Ruijter JE, Ginsel LA, von Recum AF, Jansen JA. Quantitative analysis of fibroblast morphology on microgrooved surfaces with various groove and ridge dimensions. *Biomaterials* 1996;17:2037–44. [PubMed: 8902235]
14. Dalby MJ, Riehle MO, Yarwood SJ, Wilkinson CD, Curtis AS. Nucleus alignment and cell signaling in fibroblasts: response to a micro-grooved topography. *Exp Cell Res* 2003;284:274–82. [PubMed: 12651159]
15. Deutsch J, Motlagh D, Russell B, Desai TA. Fabrication of microtextured membranes for cardiac myocyte attachment and orientation. *J Biomed Mater Res* 2000;53:267–75. [PubMed: 10813767]
16. Motlagh D, Hartman TJ, Desai TA, Russell B. Microfabricated grooves recapitulate neonatal myocyte connexin43 and N-cadherin expression and localization. *J Biomed Mater Res A* 2003;67:148–57. [PubMed: 14517872]
17. Motlagh D, Senyo SE, Desai TA, Russell B. Microtextured substrata alter gene expression, protein localization and the shape of cardiac myocytes. *Biomaterials* 2003;24:2463–76. [PubMed: 12695073]
18. Gopalan SM, Flaim C, Bhatia SN, Hoshijima M, Knoell R, Chien KR, et al. Anisotropic stretch-induced hypertrophy in neonatal ventricular myocytes micropatterned on deformable elastomers. *Biotechnol Bioeng* 2003;81:578–87. [PubMed: 12514807]
19. Zong X, Bien H, Chung CY, Yin L, Fang D, Hsiao BS, et al. Electrospun fine-textured scaffolds for heart tissue constructs. *Biomaterials* 2005;26:5330–8. [PubMed: 15814131]
20. McDevitt TC, Woodhouse KA, Hauschka SD, Murry CE, Stayton PS. Spatially organized layers of cardiomyocytes on biodegradable polyurethane films for myocardial repair. *J Biomed Mater Res A* 2003;66:586–95. [PubMed: 12918042]
21. McDevitt TC, Angello JC, Whitney ML, Reinecke H, Hauschka SD, Murry CE, et al. In vitro generation of differentiated cardiac myofibers on micropatterned laminin surfaces. *J Biomed Mater Res* 2002;60:472–9. [PubMed: 11920672]
22. Bursac N, Parker KK, Iravani S, Tung L. Cardiomyocyte cultures with controlled macroscopic anisotropy: a model for functional electrophysiological studies of cardiac muscle. *Circ Res* 2002;91:e45–54. [PubMed: 12480825]
23. Radisic M, Euloth M, Yang L, Langer R, Freed LE, Vunjak-Novakovic G. High density seeding of myocyte cells for cardiac tissue engineering. *Biotechnol Bioeng* 2003;82:403–14. [PubMed: 12632397]
24. Radisic M, Yang L, Boublik J, Cohen RJ, Langer R, Freed LE, et al. Medium perfusion enables engineering of compact and contractile cardiac tissue. *Am J Physiol Heart Circ Physiol* 2004;286:H507–16. [PubMed: 14551059]
25. Radisic M, Malda J, Epping E, Geng W, Langer R, Vunjak-Novakovic G. Oxygen gradients correlate with cell density and cell viability in engineered cardiac tissue. *Biotechnol Bioeng* 2006;93:332–43. [PubMed: 16270298]
26. Bursac N, Papadaki M, Cohen RJ, Schoen FJ, Eisenberg SR, Carrier R, et al. Cardiac muscle tissue engineering: toward an in vitro model for electrophysiological studies. *Am J Physiol* 1999;277:H433–44. [PubMed: 10444466]

27. Chehroudi B, Brunette DM. Subcutaneous microfabricated surfaces inhibit epithelial recession and promote long-term survival of percutaneous implants. *Biomaterials* 2002;23:229–37. [PubMed: 11762842]
28. Matsuzaka K, Yoshinari M, Shimono M, Inoue T. Effects of multigrooved surfaces on osteoblast-like cells in vitro: scanning electron microscopic observation and mRNA expression of osteopontin and osteocalcin. *J Biomed Mater Res A* 2004;68:227–34. [PubMed: 14704964]
29. Wu W, Lee WL, Wu YY, Chen D, Liu TJ, Jang A, et al. Expression of constitutively active phosphatidylinositol 3-kinase inhibits activation of caspase 3 and apoptosis of cardiac muscle cells. *J Biol Chem* 2000;275:40113–9. [PubMed: 11007772]
30. Schluter KD, Goldberg Y, Taimor G, Schafer M, Piper HM. Role of phosphatidylinositol 3-kinase activation in the hypertrophic growth of adult ventricular cardiomyocytes. *Cardiovasc Res* 1998;40:174–81. [PubMed: 9876330]
31. Britland S, Morgan H, Wojniak-Stodart B, Riehle M, Curtis A, Wilkinson C. Synergistic and hierarchical adhesive and topographic guidance of BHK cells. *Exp Cell Res* 1996;228:313–25. [PubMed: 8912725]
32. Charest JL, Eliason MT, Garcia AJ, King WP. Combined microscale mechanical topography and chemical patterns on polymer cell culture substrates. *Biomaterials* 2006;27:2487–94. [PubMed: 16325902]
33. Pasqui D, Rossi A, Barbucci R, Lamponi S, Gerli R, Weber E. Hyaluronan and sulphated hyaluronan micropatterns: effect of chemical and topographic cues on lymphatic endothelial cell alignment and proliferation. *Lymphology* 2005;38:50–65. [PubMed: 16184815]
34. Britland S, McCaig C. Embryonic *Xenopus* neurites integrate and respond to simultaneous electrical and adhesive guidance cues. *Exp Cell Res* 1996;226:31–8. [PubMed: 8660936]
35. Sussman MA, McCulloch A, Borg TK. Dance band on the Titanic: biomechanical signaling in cardiac hypertrophy. *Circulation Research* 2002;91:888–98. [PubMed: 12433833]
36. Nag AC. Study of non-muscle cells of the adult mammalian heart: a fine structural analysis and distribution. *Cytobios* 1980;28:41–61. [PubMed: 7428441]
37. Meyle J, Gultig K, Nisch W. Variation in contact guidance by human cells on a microstructured surface. *J Biomed Mater Res* 1995;29:81–8. [PubMed: 7713962]
38. Bursac N, Aguel F, Tung L. Multiarm spirals in a two-dimensional cardiac substrate. *Proc Natl Acad Sci U S A* 2004;101:15530–4. [PubMed: 15492227]
39. den Braber ET, de Ruijter JE, Smits HT, Ginsel LA, von Recum AF, Jansen JA. Effect of parallel surface microgrooves and surface energy on cell growth. *J Biomed Mater Res* 1995;29:511–8. [PubMed: 7622536]
40. Ohara PT, Buck RC. Contact guidance in vitro. A light, transmission, and scanning electron microscopic study. *Exp Cell Res* 1979;121:235–49. [PubMed: 571804]
41. Rakusan K, Korecky B. The effect of growth and aging on functional capillary supply of the rat heart. *Growth* 1982;46:275–81. [PubMed: 7173711]
42. Gomes PA, de Galvao KM, Mateus EF. Excitability of isolated hearts from rats during postnatal development. *J Cardiovasc Electrophysiol* 2002;13:355–60. [PubMed: 12033352]
43. Nuccitelli R. Endogenous ionic currents and DC electric fields in multicellular animal tissues. *Bioelectromagnetics* 1992;(Suppl 1):147–57. [PubMed: 1285710]
44. Clark P, Connolly P, Curtis AS, Dow JA, Wilkinson CD. Cell guidance by ultrafine topography in vitro. *J Cell Sci* 1991;99(Pt 1):73–7. [PubMed: 1757503]
45. Wodnicka M, Pierzchalska M, Bereiter-Hahn J, Kajstura J. Comparative study on effects of cytochalasins B and D on F-actin content in different cell lines and different culture conditions. *Folia Histochem Cytobiol* 1992;30:107–11. [PubMed: 1337523]
46. Leach RN, Desai JC, Orchard CH. Effect of cytoskeleton disruptors on L-type Ca channel distribution in rat ventricular myocytes. *Cell Calcium* 2005;38:515–26. [PubMed: 16137761]
47. Okada T, Otani H, Wu Y, Kyo S, Enoki C, Fujiwara H, et al. Role of F-actin organization in p38 MAP kinase-mediated apoptosis and necrosis in neonatal rat cardiomyocytes subjected to simulated ischemia and reoxygenation. *Am J Physiol Heart Circ Physiol* 2005;289:H2310–8. [PubMed: 16040713]

48. Ghosh-Choudhury N, Abboud SL, Chandrasekar B, Ghosh Choudhury G. BMP-2 regulates cardiomyocyte contractility in a phosphatidylinositol 3 kinase-dependent manner. *FEBS Lett* 2003;544:181–4. [PubMed: 12782312]
49. Vlahos CJ, Matter WF, Hui KY, Brown RF. A specific inhibitor of phosphatidylinositol 3-kinase, 2-(4-morpholinyl)-8-phenyl-4H-1-benzopyran-4-one (LY294002). *J Biol Chem* 1994;269:5241–8. [PubMed: 8106507]
50. Clark P, Connolly P, Curtis AS, Dow JA, Wilkinson CD. Topographical control of cell behaviour: II. Multiple grooved substrata. *Development* 1990;108:635–44. [PubMed: 2387239]
51. Eisenbarth E, Meyle J, Nachtigall W, Breme J. Influence of the surface structure of titanium materials on the adhesion of fibroblasts. *Biomaterials* 1996;17:1399–403. [PubMed: 8830966]
52. Tung L, Sliz N, Mulligan MR. Influence of electrical axis of stimulation on excitation of cardiac muscle cells. *Circ Res* 1991;69:722–30. [PubMed: 1873867]
53. Sharp WW, Terracio L, Borg TK, Samarel AM. Contractile activity modulates actin synthesis and turnover in cultured neonatal rat heart cells. *Circulation Research* 1993;73:172–83.
54. McDermott P, Daood M, Klein I. Contraction regulates myosin synthesis and myosin content of cultured heart cells. *Am J Physiol* 1985;249:H763–9. [PubMed: 2931998]
55. Cameron LA, Giardini PA, Soo FS, Theriot JA. Secrets of actin-based motility revealed by a bacterial pathogen. *Nat Rev Mol Cell Biol* 2000;1:110–9. [PubMed: 11253363]
56. Cooper JA, Schafer DA. Control of actin assembly and disassembly at filament ends. *Curr Opin Cell Biol* 2000;12:97–103. [PubMed: 10679358]
57. Toker A, Cantley LC. Signalling through the lipid products of phosphoinositide-3-OH kinase. *Nature* 1997;387:673–6. [PubMed: 9192891]
58. McMullen JR, Shioi T, Huang WY, Zhang L, Tarnavski O, Bisping E, et al. The insulin-like growth factor 1 receptor induces physiological heart growth via the phosphoinositide 3-kinase(p110alpha) pathway. *J Biol Chem* 2004;279:4782–93. [PubMed: 14597618]
59. McMullen JR, Shioi T, Zhang L, Tarnavski O, Sherwood MC, Kang PM, et al. Phosphoinositide 3-kinase(p110alpha) plays a critical role for the induction of physiological, but not pathological, cardiac hypertrophy. *Proc Natl Acad Sci U S A* 2003;100:12355–60. [PubMed: 14507992]
60. Zhao M, Bai H, Wang E, Forrester JV, McCaig CD. Electrical stimulation directly induces pre-angiogenic responses in vascular endothelial cells by signaling through VEGF receptors. *Journal of Cell Science* 2004;117:397–405. [PubMed: 14679307]
61. Zhao M, Song B, Pu J, Wada T, Reid B, Tai G, et al. Electrical signals control wound healing through phosphatidylinositol-3-OH kinase-gamma and PTEN. *Nature* 2006;442:457–60. [PubMed: 16871217]
62. Janmey PA. The cytoskeleton and cell signaling: component localization and mechanical coupling. *Physiol Rev* 1998;78:763–81. [PubMed: 9674694]
63. Courtney T, Sacks MS, Stankus J, Guan J, Wagner WR. Design and analysis of tissue engineering scaffolds that mimic soft tissue mechanical anisotropy. *Biomaterials* 2006;27:3631–8. [PubMed: 16545867]
64. Stankus JJ, Guan J, Wagner WR. Fabrication of biodegradable elastomeric scaffolds with sub-micron morphologies. *J Biomed Mater Res A* 2004;70:603–14. [PubMed: 15307165]
65. Shimizu T, Yamato M, Isoi Y, Akutsu T, Setomaru T, Abe K, et al. Fabrication of pulsatile cardiac tissue grafts using a novel 3- dimensional cell sheet manipulation technique and temperature-responsive cell culture surfaces. *Circulation Research* 2002;90:e40–e8. [PubMed: 11861428]



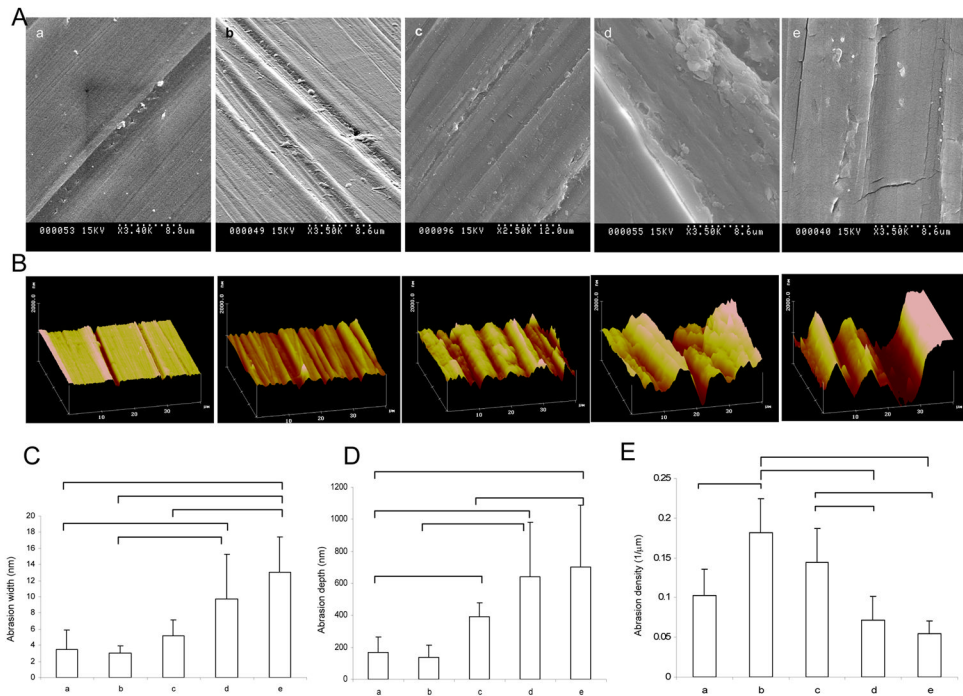


**Figure 1. Abraded surfaces**

A) SEM images of the abraded surfaces B) AFM images of the abraded surfaces C) Abrasion width as estimated by AFM. D) Abrasion depth as estimated by AFM. E) Abrasion density as estimated by AFM. The letters a, b, c, d and e represent abrasions made by lapping paper of grain size 1, 9, 12, 40 and 80 μm respectively. ( $p < 0.05$ , Dunn's test).

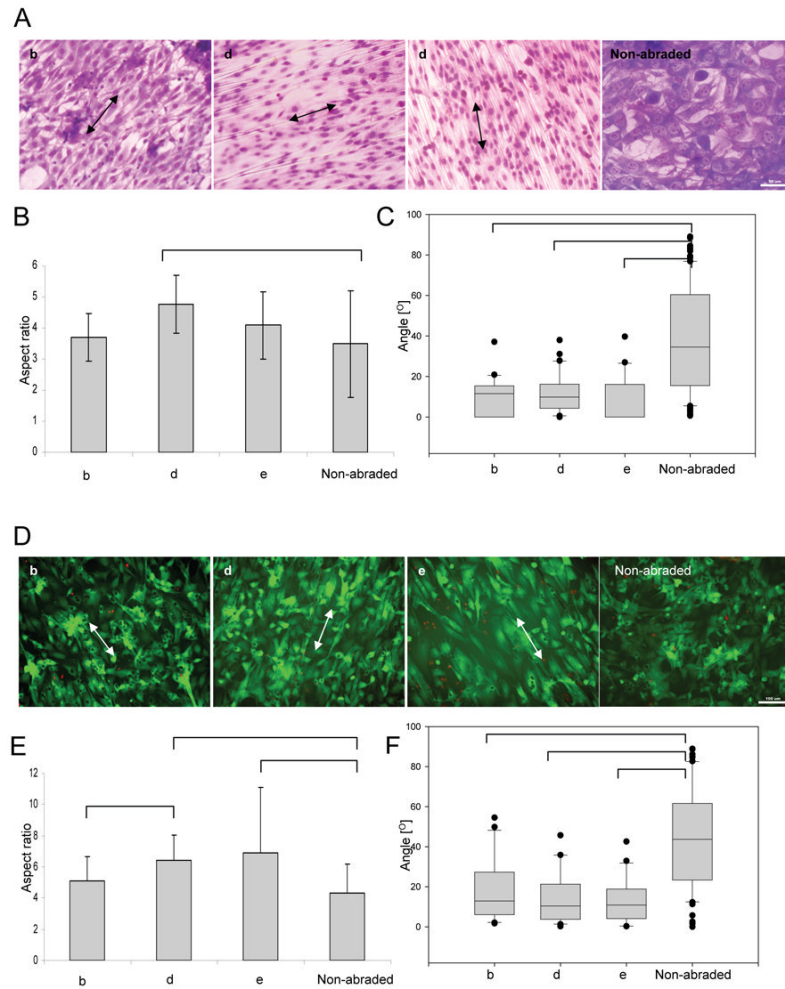


**Figure 2. Elongation and orientation of fibroblasts (A-C) and cardiomyocytes (D-E) cultivated on abraded and non-abraded surfaces**

Abraded surfaces were created by lapping paper with grain sizes of 9µm, 40µm and 80µm respectively (b, d, e). Aspect ratio is defined as the ratio between the long and the short axis of the cell. Orientation angle is defined as the angle between the long axis of the cell and the direction of abrasion. Arrows indicate direction of abrasion. For cells cultured on non-abraded surfaces orientation angle is measured with respect to the horizontal axis of the image. A) Giemsa staining of fibroblasts. (Scale bar: 100µm for b, d, e and 50µm for non-abraded). B) Elongation of fibroblasts as measured by the aspect ratio. C) Alignment of fibroblasts as measured by the orientation angle (box plots). D) Live/dead (green/red) staining of cardiomyocytes. (Scale bar: 100µm) E) Elongation of cardiomyocytes as measured by the aspect ratio. F) Alignment of cardiomyocytes as measured by the orientation angle (box plots).

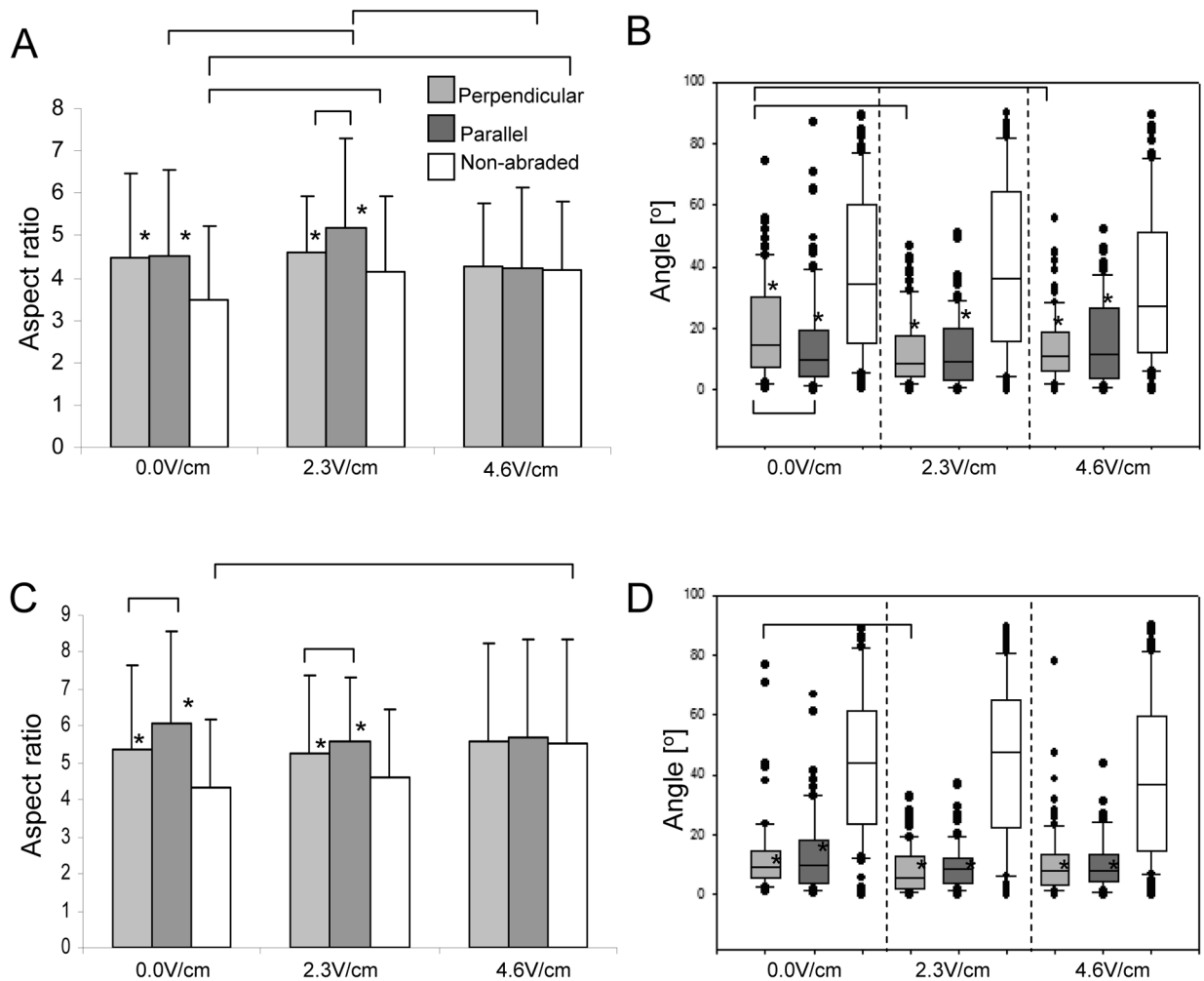


**Figure 3. Interactive effects of topographical cues and electrical field stimulation on fibroblasts (A,B) and cardiomyocytes (C,D)**

Electrical field stimulation using square pulses 1ms duration, 1Hz and 2.3V/cm or 4.6V/cm was initiated 24hr after cell seeding and maintained for additional 72hr. Abraded surfaces were placed between the electrodes so that the abrasions were either perpendicular or parallel to the field lines. A) Elongation of fibroblasts as measured by the aspect ratio. B) Alignment of fibroblasts as measured by the orientation angle (box plots). C) Elongation of cardiomyocytes as measured by the aspect ratio. D) Alignment of cardiomyocytes as measured by the orientation angle (box plots). Total N=2-3 independent samples (cover slips) per group; 30-90 cells were analysed per group. ( $p < 0.05$  was considered significant). \*significantly different than non-abraded surface at identical stimulation voltage.

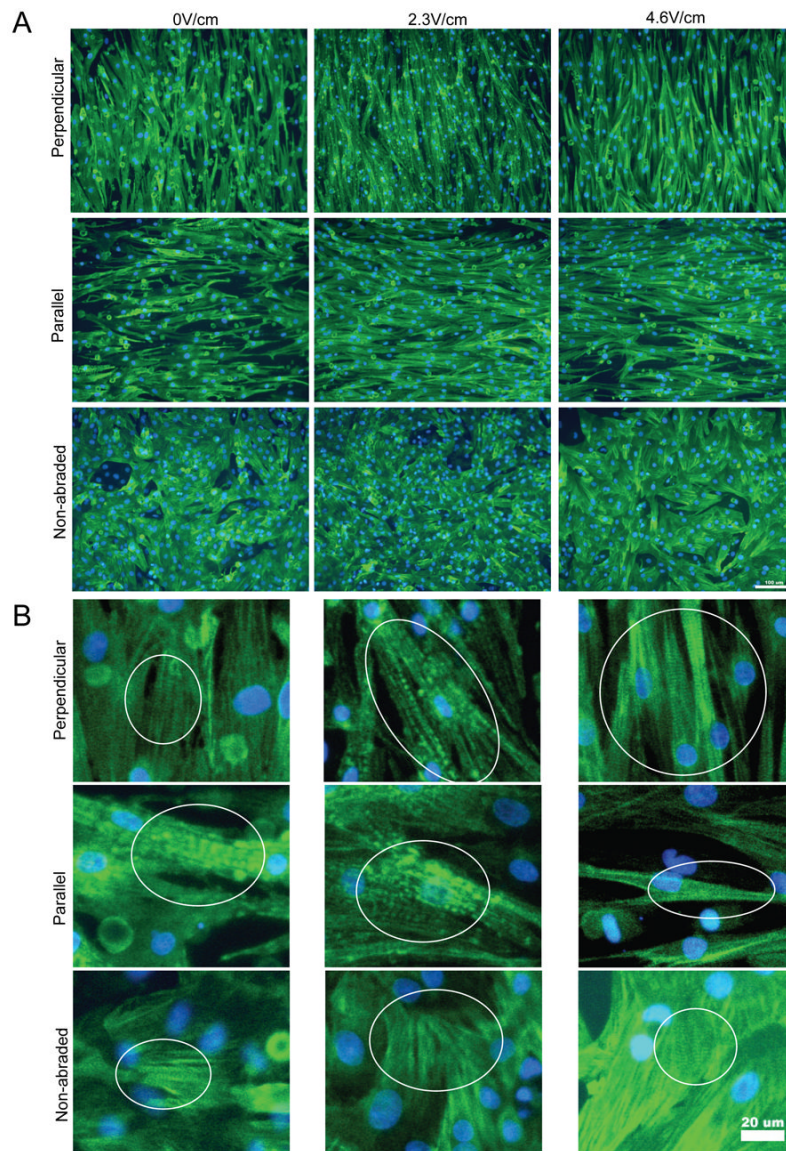


**Figure 4. Immunostaining for cardiac Troponin I of cardiomyocytes cultivated in the presence of electrical field stimulation on abraded surfaces**

A) Orientation and morphology of cells expressing cardiac troponin I. Scale bar 100 $\mu$ m. B) Higher magnification images indicate the presence of contractile apparatus (cross-striations). Scale bar 20 $\mu$ m.

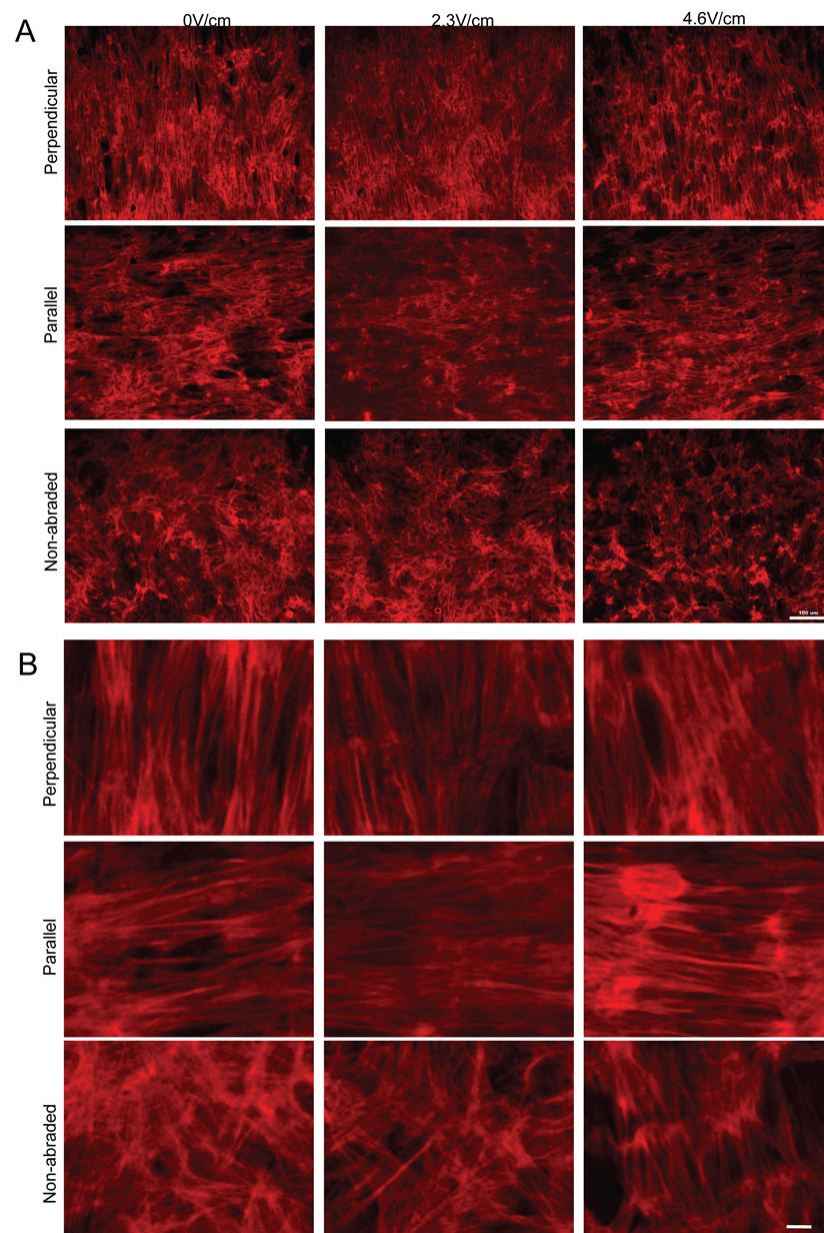


**Figure 5. Actin cytoskeleton in cardiomyocytes cultivated in the presence of electrical field stimulation on abraded surfaces**

A) Orientation and morphology of cells stained with phalloidin-TRITC. Scale bar 100µm. B) Higher magnification images indicate orientation of actin microfilaments. Scale bar 10µm.

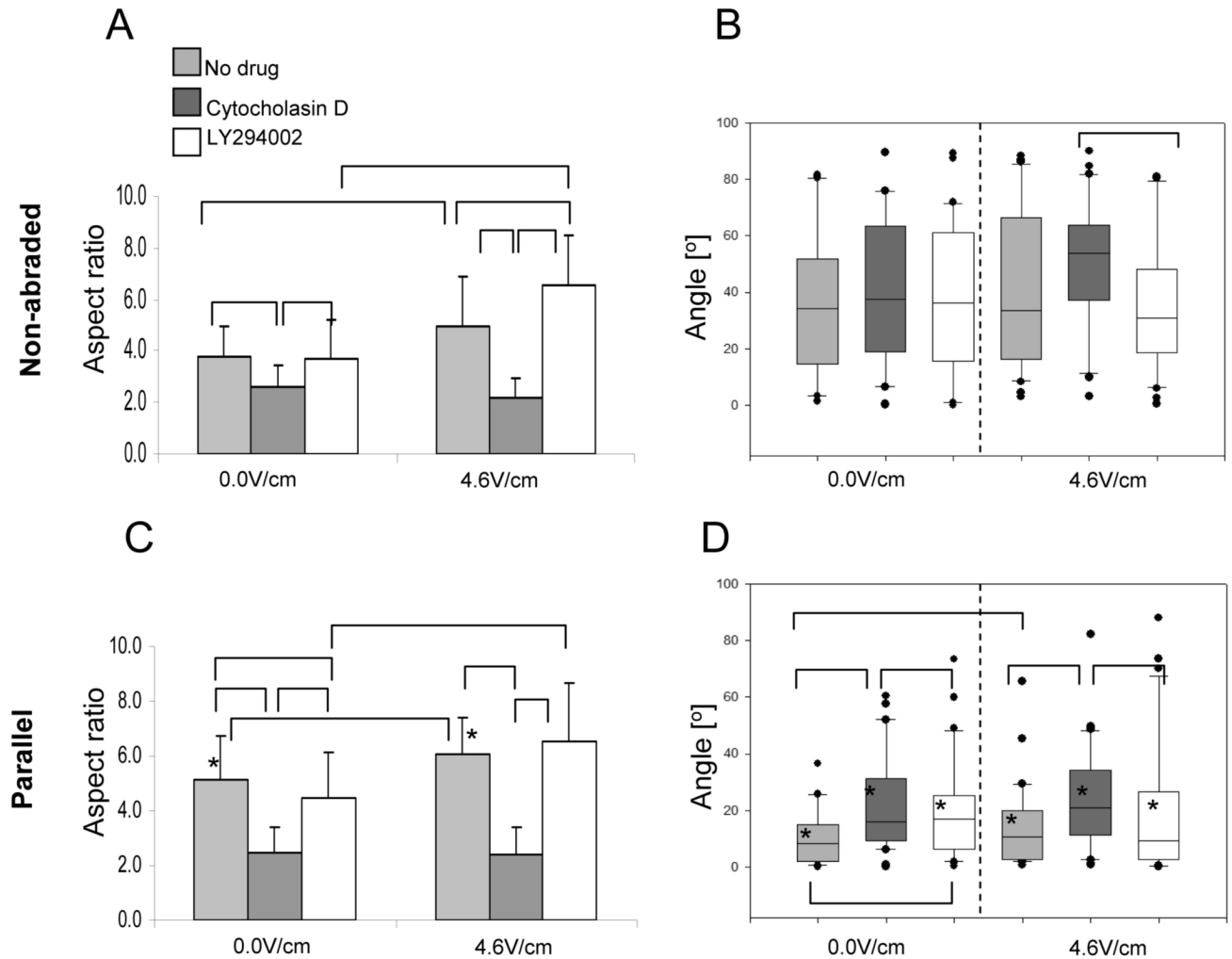


**Figure 6. Effects of pharmacological agents on elongation (A, C) and orientation (B, D) of cardiomyocytes cultivated on non-abraded (A, B) and abraded (C, D) surfaces**  
 A) Elongation of cardiomyocytes on non-abraded surfaces B) Alignment of cardiomyocytes on non-abraded surfaces C) Elongation of cardiomyocytes on abrasions placed parallel to the field lines D) Alignment of cardiomyocytes on abrasions placed parallel to the field lines N=2-3 independent samples per treatment; 30 cells were analyzed per treatment. ( $p < 0.05$  was considered significant). \*significantly different than non-abraded surface at identical stimulation voltage.

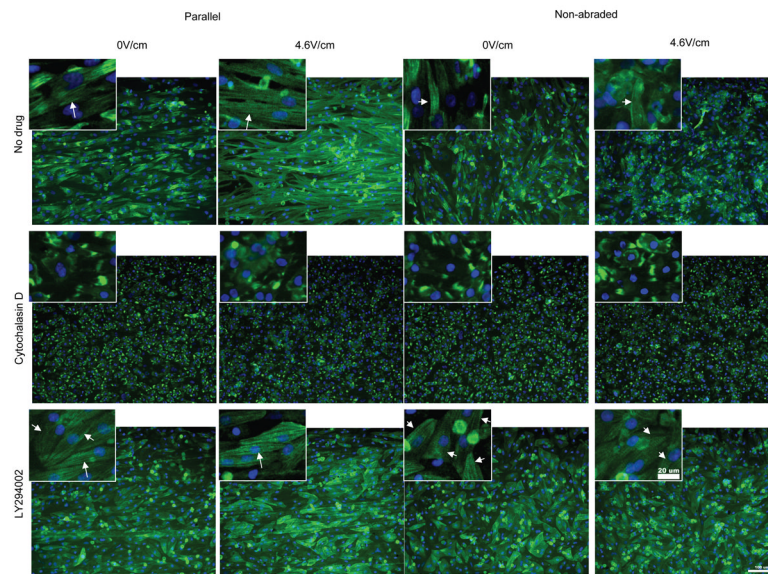


**Figure 7. Immunostaining for cardiac Troponin I of cardiomyocytes treated with pharmacologic agents**

Main panels indicate the orientation and morphology of cells expressing cardiac troponin I. Scale bar 100 $\mu$ m. Insets: Higher magnification images indicate the presence of contractile apparatus (cross-striations) in No-drug and LY294002 group (arrows). Scale bar 20 $\mu$ m.

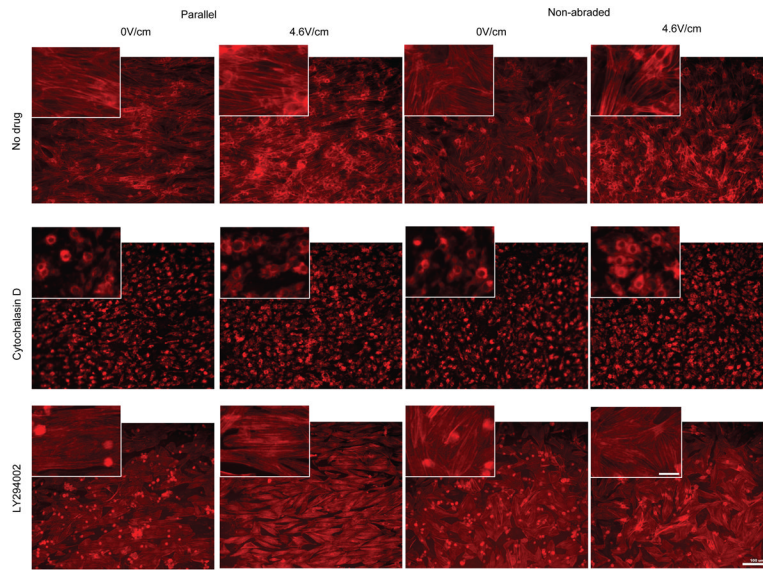


**Figure 8. Actin cytoskeleton in cardiomyocytes treated with pharmacologic agents**  
 Main panels indicate the orientation and morphology of cells expressing stained with phalloidin-TRITC. Scale bar 100µm. Insets: Higher magnification images indicate orientation of actin microfilaments. Scale bar 20µm.



Table 1

**Contractile properties of cardiomyocytes as a function of surface abrasions and electrical field stimulation**

Cardiomyocytes were seeded on vinyl cover slips (abraded and non-abraded) and cultivated for 24 hr without field stimulation to allow for the cell attachment. Contractile properties at 24 hr in culture were as follows: After 24 hr field stimulation was initiated using square pulses 1ms duration, 1 Hz with two different field strengths: 2.3V/cm and 4.6V/cm. Abraded surfaces were placed between the carbon electrodes so that the abrasions either perpendicular or parallel to the field lines. The cells were cultivated for addition 72 hr followed by evaluation of contractile properties (ET and MCR).

| Contractile properties at 24 hr in culture: |                                  | 0.0V/cm                          |                 | 2.3V/cm                          |                                    | 4.6V/cm                            |                 |
|---|----------------------------------|----------------------------------|-----------------|----------------------------------|------------------------------------|------------------------------------|-----------------|
|   | Perpendicular                    | Parallel                         | Non-abraded     | Perpendicular                    | Parallel                           | Perpendicular                      | Non-abraded     |
| ET (V/cm)                                   | 2.8 ± 0.7 (18/18)                | 2.6 ± 0.5 (18/20)                | 1.7 ± 0.4 (6/6) | 1.9 ± 0.4 <sup>&amp;</sup> (5/6) | 1.9 ± 0.6 <sup>&amp;</sup> (5/6)   | 1.9 ± 0.9 <sup>&amp;</sup> (5/6)   | 2.6 ± 1.5 (8/8) |
| MCR (Hz)                                    | 3.7 ± 1.0* (17/18)               | 4.2 ± 1.1 (18/20)                | 3.5 ± 1.5 (3/6) | 3.6 ± 1.6 (5/6)                  | 2.7 ± 1.1 <sup>&amp;</sup> § (5/6) | 2.6 ± 0.4 <sup>&amp;</sup> * (5/6) | 3.9 ± 1.3 (8/8) |
| Contractile properties at 96 hr in culture: |                                  | 0.0V/cm                          |                 | 2.3V/cm                          |                                    | 4.6V/cm                            |                 |
| Type of stimulation                         | Perpendicular                    | Parallel                         | Non-abraded     | Perpendicular                    | Parallel                           | Perpendicular                      | Non-abraded     |
| ET (V/cm)                                   | 2.2 ± 0.5 <sup>&amp;</sup> (3/4) | 2.0 ± 0.4 <sup>&amp;</sup> (7/7) | 1.7 ± 0.4 (6/6) | 1.9 ± 0.4 <sup>&amp;</sup> (5/6) | 1.9 ± 0.6 <sup>&amp;</sup> (5/6)   | 1.9 ± 0.9 <sup>&amp;</sup> (5/6)   | 2.6 ± 1.5 (8/8) |
| MCR (Hz)                                    | 2.7 ± 0.3 <sup>&amp;</sup> (3/4) | 2.8 ± 0.3 <sup>&amp;</sup> (5/7) | 3.5 ± 1.5 (3/6) | 3.6 ± 1.6 (5/6)                  | 2.7 ± 1.1 <sup>&amp;</sup> § (5/6) | 2.6 ± 0.4 <sup>&amp;</sup> * (5/6) | 3.9 ± 1.3 (8/8) |

<sup>&</sup> significantly different than the same group at 24hr

\* significantly different than non-abraded at the same time point and stimulation regime

§ significantly different than parallel at 4.6V/cm

**Effect of pharmacologic agents on contractile properties of cardiomyocytes cultivated in the presence of electrical field stimulation (0V/cm or 4.6V/cm) on non-abraded and abraded surfaces placed parallel to the field lines**

Cardiomyocytes were seeded on polyvinyl cover slips (abraded and non-abraded) and cultivated for 24 hr without field stimulation to allow for the cell attachment. After 24 hr pharmacologic agents (Cytochalasin D, 1 $\mu$ g/ml and LY294002, 50 $\mu$ M) were added to the cover slips and field stimulation was initiated using square pulses 1ms duration, 1 Hz and 4.6V/cm. The abraded cover-slips were placed such that the abrasions were parallel to the field lines. Field stimulation in the presence of pharmacologic agents was maintained for additional 72 hr. The ET and MCR were measured at 24 hr prior to addition of pharmacologic agents and the averages were: 2.6 $\pm$ 0.1V/cm and 4.1 $\pm$ 0.2Hz for abraded surfaces; 2.6 $\pm$ 0.1V/cm and 3.8 $\pm$ 0.2 Hz for non-abraded surfaces. N/A indicates that the sample could not be induced to contract by field stimulation at all, or only isolated cells (less than 75% of area) were responding. The numbers in brackets indicate the number of samples that were successfully paced/number of samples tested.

| Type of stimulation | 0V/cm          |                          | 4.6V/cm                  |                          |
|---------------------|----------------|--------------------------|--------------------------|--------------------------|
|                     | Non-abraded    | Parallel                 | Non-abraded              | Parallel                 |
| ET (V/cm)           | No drug        | 1.7 $\pm$ 0.2 $\&$ (3/3) | 1.8 $\pm$ 0.3 $\&$ (3/3) | 2.1 $\pm$ 0.6 (3/3)      |
|                     | Cytochalasin D | N/A (0/3)                | N/A (0/3)                | N/A (0/3)                |
| MCR (Hz)            | LY294002       | N/A (0/3)                | N/A (0/3)                | N/A (0/3)                |
|                     | No drug        | 3.0 $\pm$ 0.1 $\&$ (3/3) | 3.0 $\pm$ 0.2 $\&$ (3/3) | 3.1 $\pm$ 0.4 (3/3) $\&$ |
|                     | Cytochalasin D | N/A (0/3)                | N/A (0/3)                | N/A (3/3)                |
|                     | LY294002       | N/A (0/3)                | N/A (0/3)                | N/A (0.3)                |

$\&$  significantly different than the same group at 24hr